Scheme I. In 3 the tenth metal atom remains attached to the complex by a hydride-bridged metal–metal bond and two μ_3-η^2 carbonyl ligands serving as four-electron donors. This μ_3-η^2 coordination type A is new although

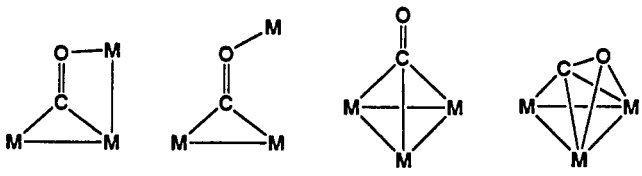

A B C D

there are related examples of μ_3-η^2 carbonyl ligands where the oxygen-coordinated metal atom is not directly bonded to the other metal atoms, B.[21,22] Other examples of triply bridging carbonyl ligands include the μ_3-η^1 C,[22] a two-electron donor, and the μ_3-η^2 D, which serves as a six-electron donor.[23]

In the formation of 4 one metal atom was completely removed from the cluster. It seems likely that compound 3 could represent an intermediate species traversed in the course of the degradation of 2 to 4. It is possible that the product obtained from the reaction of 1 with CO may eventually prove to be an analog of 4.

Acknowledgment. These studies were supported by the National Science Foundation under Grant No. CHE-8919786. We wish to thank Dr. Istvan Horvath of Exxon Research and Engineering Co. for providing a sample of ^{13}CO for use in the labeling studies.

Supplementary Material Available: Tables of hydrogen atom parameters, anisotropic thermal parameters, and bond distances and angles for all four structural analyses (43 pages). Ordering information is given on any current masthead page.

OM920347D

(21) (a) Cotton, F. A.; Schwotzer, W. *J. Am. Chem. Soc.* **1983**, *105*, 4955. (b) Chisholm, M. H.; Hoffmann, D. M.; Huffman, J. C. *Organometallics* **1985**, *4*, 986.

(22) Horwitz, C. P.; Shriver, D. F. *Adv. Organomet. Chem.* **1984**, *23*, 219 and references therein.

(23) Herrmann, W. A.; Biersack, H.; Ziegler, M. L.; Weidenhammer, K.; Siegel, R.; Rehder, D. *J. Am. Chem. Soc.* **1981**, *103*, 1692.

Syntheses of $(\mu$-H)FeRu$_2(\mu$-CX)(CO)$_{10}$ (X = OMe, NMe$_2$) and $(\mu$-H)$_3$FeRu$_2(\mu_3$-COMe)(CO)$_9$. Ligand Substitution on $(\mu$-H)Fe$_n$Ru$_{3-n}(\mu$-CNMe$_2$)(CO)$_{10}$ (n = 1, 3)

Derrick S. Parfitt, Jeffrey D. Jordan, and Jerome B. Keister*

Department of Chemistry, University at Buffalo, State University of New York, Buffalo, New York 14214

Received May 19, 1992

The new clusters HFeRu$_2(\mu$-CX)(CO)$_{10}$ (X = OMe, NMe$_2$) have been prepared in low yield by metal fragment exchange. Hydrogenation of HFeRu$_2(\mu$-COMe)(CO)$_{10}$ yields H$_3$FeRu$_2(\mu_3$-COMe)(CO)$_9$. For X = NMe$_2$ reaction with PPh$_3$ gives HFeRu$_2(\mu$-CNMe$_2$)(CO)$_9$(PPh$_3$) and HFeRu$_2(\mu$-CNMe$_2$)(CO)$_8$(PPh$_3$)$_2$ with all substitutions on Ru. Kinetic studies of substitution by PPh$_3$ on HFe$_3(\mu$-CNMe$_2$)(CO)$_{10}$ and on HFeRu$_2(\mu$-CNMe$_2$)(CO)$_{10}$ found that the mechanism involves rate-determining CO dissociation. The order of relative rates for substitution, FeRu$_2$ > Fe$_3$ > Ru$_3$, suggests that CO dissociation occurs from Fe. The higher rate for the mixed-metal cluster is attributed to labilization of the Fe center by the Ru "ligand".

The reactivities of mixed-metal clusters provide an opportunity to probe mechanisms.[1] We have used the relative reactivities of the clusters HRu$_{3-n}$Os$_n(\mu$-COMe)(CO)$_{10}$ and H$_3$Ru$_{3-n}$Os$_n(\mu_3$-COMe)(CO)$_9$ to determine the number of metal atoms which are involved in the transition state for reductive elimination of hydrogen from the latter clusters.[2] For both CO dissociation and H_2 elimination the relative rates are in the order Ru$_3$ > Ru$_2$Os > RuOs$_2$ ≫ Os$_3$; the mixed-metal clusters are intermediate in reactivity between, but with rates closer to that of the most reactive of, the two homometallic analogs. However, the reactivities of mixed Ru/Fe trinuclear clusters have been shown to be different. For CO dissociation from Fe$_{3-n}$Ru$_n$(CO)$_{12}$ the mixed-metal clusters were the most reactive, the order of relative rates being Fe$_2$Ru (21) > FeRu$_2$ (12) > Fe$_3$ (4.6) > Ru$_3$ (1);[3] however, the site of substitution for the mixed Fe/Ru clusters is on Ru.[3,4] Complicating features are the lack of structural similarity throughout the series, with the number of bridging carbonyl ligands decreasing as the Ru content increases and only a small range in rate constants. Mixed Fe/Ru clusters have also been shown to be more active catalysts for the water gas shift reaction than the homometallic analogs.[5]

We report here the syntheses of the new mixed-metal alkylidyne clusters HFeRu$_2(\mu$-CX)(CO)$_{10}$ (X = OMe, NMe$_2$) and their reactions with H_2 (X = OMe) and with

(1) (a) Gladfelter, W. L.; Geoffroy, G. L. *Adv. Organomet. Chem.* **1980**, *18*, 207. (b) Roberts, D. A.; Geoffroy, G. L. In *Comprehensive Organometallic Chemistry*; Wilkinson, G., Ed.; Pergamon Press: Oxford, U.K., 1982; Vol. 6, p 763.

(2) Keister, J. B.; Onyeso, C. C. O. *Organometallics* **1988**, *7*, 2364.

(3) (a) Shojaie, R.; Atwood, J. D. *Inorg. Chem.* **1987**, *26*, 2199. (b) Shojaie, A.; Atwood, J. D. *Organometallics* **1985**, *4*, 187.

(4) Venalainen, T., Pakkanen, T. *J. Organomet. Chem.* **1984**, *266*, 269.

(5) (a) Ford, P. C.; Rinker, R. G.; Ungermann, C.; Laine, R. M.; Landis, V.; Moya, S. A. *J. Am. Chem. Soc.* **1978**, *100*, 4595. (b) Ungermann, C.; Landis, V.; Moya, S. A.; Cohen, H.; Walker, H.; Pearson, R. G.; Rinker, R. G.; Ford, P. C. *Ibid.* **1979**, *101*, 5922.

0276-7333/92/2311-4009$03.00/0

PPh_3 (X = NMe_2). This study confirms the higher reactivity for ligand substitution of mixed Fe/Ru clusters, but not for hydrogen elimination, and provides an example of bimetallic participation in the mechanism of ligand substitution.

Experimental Section

$HM_3(\mu\text{-}CX)(CO)_{10}$ complexes (M = Ru, X = OMe[6] and NMe_2;[7] M = Fe, X = NMe_2[8]) were prepared by published procedures. $Fe(CO)_5$ was purchased from Aldrich and was used without further purification. All experiments were conducted under a nitrogen atmosphere with Schlenk techniques, but workups of products were conducted in air. IR spectra were recorded on a Beckman 4250 infrared spectrophotometer in KBr cells with a 0.5-mm path length. ^1H NMR spectra were recorded on a Varian Gemini 300-MHz instrument. $^{31}P\{^1H\}$ NMR spectra were taken on a Varian 400-MHz instrument; ^{31}P chemical shifts are relative to phosphoric acid. ^{13}C NMR spectra were recorded on a Varian Gemini 300-MHz or VXR 400-MHz instrument; $Cr(acac)_3$ was added as a relaxation agent. Mass spectra were obtained by using a VG 70-SE instrument. Analyses were performed by Schwarzkopf Microanalytical Laboratory (Woodside, NY) and Galbraith Laboratories (Knoxville, TN).

Synthesis of $HFeRu_2(\mu\text{-}COMe)(CO)_{10}$. $HRu_3(\mu\text{-}COMe)(CO)_{10}$ (200 mg, 0.32 mmol) and $Fe(CO)_5$ (200 μL, 1.96 mmol) in 10 mL of cyclohexane were placed in a 50-mL Schlenk flask under nitrogen. The solution was heated to 70 °C for 2 h. The solvent and unreacted $Fe(CO)_5$ were removed by vacuum transfer. The products were separated by thin-layer chromatography (Kieselgel 60G) using cyclohexane as the eluting solvent. The products in order of elution were $H_4Ru_4(CO)_{12}$ (6.5 mg, 4%), $HRu_3(COMe)(CO)_{10}$ (125.3 mg, 79%), $HFeRu_2(COMe)(CO)_{10}$ (9.6 mg, 6%), $H_2Ru_4(CO)_{13}$ (7.9 mg, 5%), and $HRu_4(COMe)(CO)_{12}$ (9.2 mg, 6%).[9]

$HFeRu_2(\mu\text{-}COMe)(CO)_{10}$. ^1H NMR ($CDCl_3$, 25 °C): −14.32 (s, 1 H) and 4.61 (s, 3 H) ppm, isomer 1, 45%; 4.65 (s, 3 H) and −16.85 (s, 1 H) ppm, isomer 2, 55%. IR (C_6H_{12}): 2103 (vw), 2070 (m), 2050 (s), 2040 (sh, s), 2038 (vs), 2021 (sh, s), 2008 (m), 1999 (m), 1989 (m), and 1964 (w) cm^{-1}. MS (EI): m/z 583 ($^{102}Ru_2{}^{56}Fe$). Anal. Calcd for $H_4C_{12}O_{11}Ru_2Fe$: C, 24.76; H, 0.69. Found: C, 24.44; H, 0.73.

Synthesis of $H_3FeRu_2(\mu_3\text{-}COMe)(CO)_9$. $HFeRu_2(\mu\text{-}COMe)(CO)_{10}$ (10 mg, 0.017 mmol) in 15 mL of cyclohexane was placed in a three-necked, 50-mL flask equipped with condenser and gas inlet tube, and the solution was heated at 70 °C for 2 h with H_2 bubbling through. All volatile components were then removed by vacuum transfer. The nonvolatile residue was purified by thin-layer chromatography (Kieselgel 60G) using cyclohexane as the eluting solvent. The only product isolated was $H_3FeRu_2(\mu_3\text{-}COMe)(CO)_9$ (8 mg, 80%).

$H_3FeRu_2(\mu_3\text{-}COMe)(CO)_9$. IR ($C_6H_{12}$): 2104 (vw), 2077 (s), 2059 (s), 2035 (vs), 2022 (m), 2011 (s), and 1988 (w) cm^{-1}. ^1H NMR ($CDCl_3$, 25 °C): −18.08 (t, 1 H_A), −20.05 (d, 2 H_B), and 4.04 (s, 3 H) ppm, J_{AB} = 3.0 Hz. ^{13}C NMR ($CDCl_3$, 25 °C): 266.5 (1 C, μ_3-C), 207.0 (2 C, eq FeCO), 206.4 (1 C, ax FeCO), 191.2 (2 C, RuCO), 190.2 (2 C, RuCO), 190.0 (2 C, RuCO), and 68.4 (1 C, Me) ppm. MS(EI): m/z 558 ($^{102}Ru_2{}^{56}Fe$). Anal. Calcd for $C_{11}H_6O_{10}FeRu_2$: C, 23.75; H, 1.08. Found: C, 23.46; H, 1.10.

Carbonylation of $H_3FeRu_2(\mu_3\text{-}COMe)(CO)_9$. A 1:1 mixture of $H_3FeRu_2(\mu_3\text{-}COMe)(CO)_9$ and $H_3Ru_3(\mu_3\text{-}COMe)(CO)_9$, total 43.2 mg, was placed with 20 mL of hexanes in a 50-mL Schlenk flask equipped with a consenser, stirbar, and CO inlet. The solution was heated to 55 °C for 2.5 h before all volatile components were removed by a rotary evaporator. The products were separated by thin-layer chromatography (Kieselgel 60G) using hexanes as the eluting solvent. Five bands were found and characterized by IR spectroscopy: Band one, light yellow, 1.4 mg, $H_4Ru_4(CO)_{12}$; band two, yellow, 2.3 mg, $HRu_3(\mu\text{-}COMe)(CO)_{10}$; band three, yellow-orange, 10.0 mg, $HFeRu_2(\mu\text{-}COMe)(CO)_{10}$; band four, red, 2.9 mg, $H_3FeRu_2(\mu_3\text{-}COMe)(CO)_9$; band five, orange, 19.9 mg, $H_3Ru_3(\mu_3\text{-}COMe)(CO)_9$.

Synthesis of $HFeRu_2(\mu\text{-}CNMe_2)(CO)_{10}$. $HRu_3(\mu\text{-}CNMe_2)(CO)_{10}$ (200 mg, 0.312 mmol) and $Fe(CO)_5$ (400 μL, 3.92 mmol) with 10 mL of cyclohexane were placed in a 50-mL Schlenk flask equipped with a condenser and nitrogen inlet. The solution was heated at 70 °C for 1.5 h. All volatile components were then removed by vacuum transfer. Thin-layer chromatography using cyclohexane as the eluting solvent gave the following bands: $H_4Ru_4(CO)_{12}$ (4.5 mg, 2%); $H_2Ru_4(CO)_{13}$ (1.9 mg, 1%); $HRu_3(\mu\text{-}CNMe_2)(CO)_{10}$ (129.4 mg, 65%); $HFeRu_2(\mu\text{-}CNMe_2)(CO)_{10}$ (33.5 mg, 18%); $HRu_4(\mu_4\text{-}CNMe_2)(CO)_{12}$ (1.9 mg, 1%).[10]

$HFeRu_2(\mu\text{-}CNMe_2)(CO)_{10}$. IR ($C_6H_{12}$): 2093 (w), 2057 (s), 2048 (s), 2028 (m), 2021 (m), 2004 (s), 1992 (m), 1969 (w), and 1955 (w) cm^{-1}. ^1H NMR ($CDCl_3$, 25 °C): −14.30 (s, 1 H), and 3.84 (s, 6 H) ppm. $^{13}C\{^1H\}$ NMR ($CDCl_3$, −60 °C): 309.7 (1 C, $CNMe_2$), 220.0 (1 C, ax FeCO), 220.1 (1 C, ax FeCO), 210.5 (2 C, eq FeCO), 199.9 (2 C, RuCO), 197.0 (2 C, RuCO), 191.1 (2 C, RuCO), 54.2 (2 C, Me) ppm. MS (EI): m/z 597 ($^{102}Ru_2{}^{56}Fe$). Anal. Calcd for $H_7C_{13}O_{10}NRu_2Fe$: C, 26.23; H, 1.19. Found: C, 26.10; H, 1.14.

Reaction of $HFeRu_2(\mu\text{-}CNMe_2)(CO)_{10}$ with PPh_3. $HFeRu_2(\mu\text{-}CNMe_2)(CO)_{10}$ (30.1 mg, 0.0506 mmol) and PPh_3 (17.6 mg, 0.0496 mmol) in $CDCl_3$ were placed in a NMR tube under a nitrogen atomosphere and allowed to react for 24 h. The solution was separated by thin-layer chromatography using cyclohexane/dichloromethane (5:1 v/v) as the eluting agent. The bands in the following order were found: $HRu_3(\mu\text{-}CNMe_2)(CO)_{10}$ (4.6 mg, 13%); $HFeRu_2(\mu\text{-}CNMe_2)(CO)_{10}$ (6.7 mg, 21%); $HRu_3(\mu\text{-}CNMe_2)(CO)_9(PPh_3)$ (4.0 mg, 13%); $HFeRu_2(\mu\text{-}CNMe_2)(CO)_9(PPh_3)$ (16.1 mg, 51%).

$HRu_3(\mu\text{-}CNMe_2)(CO)_9(PPh_3)$.[7a] IR ($C_6H_{12}$): 2077 (m), 2036 (s), 2008 (s), 1994 (m), 1983 (m), and 1964 (w) cm^{-1}. ^1H NMR ($CDCl_3$, 25 °C): b-e isomer, 2.80 (s, 3 H), 3.59 (s, 3 H, and −14.35 (d, J_{PH} = 8.4 Hz, 1 H) ppm; n-e isomer, 3.71 (s, 6 H) and −14.25 (d, 1 H, J_{PH} = 3 Hz) ppm. $^{31}P\{^1H\}$ NMR ($CDCl_3$, 25 °C): b-e isomer, 39.1 ppm; n-e isomer, 37.0 ppm.

$HFeRu_2(\mu\text{-}CNMe_2)(CO)_9(PPh_3)$. IR ($C_6H_{12}$): 2072 (m), 2030 (s), 2008 (s), 1996 (s), 1989 (sh), and 1965 (s) cm^{-1}. ^1H NMR ($CDCl_3$, 25 °C): 7.3 (br, 15 H), 2.86 (s, 3 H), 3.60 (s, 3 H), and −13.76 (d, J_{PH} = 8.1 Hz, 1 H) ppm. $^{31}P\{^1H\}$ NMR ($CDCl_3$, 25 °C): 41.5 (s) ppm. $^{13}C\{^1H\}$ NMR ($CDCl_3$, −60 °C): 317.2 (s, 1 C, CNR_2), 228.7 (s, 1 C, ax FeCO), 222.4 (s, 1 C, ax FeCO), 220.2 (s, 1 C, eq FeCO), 210.0 (s, 1 C, eq Fe), 206.6 (d, J_{PC} = 9.5 Hz, 1 C, $Ru(CO)_2PR_3$), 202.0 (d, J_{PC} = 6.7 Hz, 1 C, $Ru(CO)_2PR_3$), 200.8 (s, 1 C, $Ru(CO)_3$), 198.4 (s, 1 C, $Ru(CO)_3$), 190.2 (s, 1 C, $Ru(CO)_3$), 54.1 (s, 1 C, Me), and 52.1 (s, 1 C, Me) ppm. Anal. Calcd for $C_{30}H_{22}FeNPO_9Ru_2$: C, 43.44; H, 2.67. Found: C, 43.26; H, 2.59.

$HFeRu_2(\mu\text{-}CNMe_2)(CO)_8(PPh_3)_2$. IR ($C_6H_{12}$): 2070 (w), 2056 (w), 2043 (w), 2029 (m), 2006 (m), 1994 (vs, br), 1965 (s, br), and 1938 (w) cm^{-1}. ^1H NMR ($CDCl_3$, 25 °C): 7.4 (m, 30 H), 3.62 (s, 3 H), 2.70 (s, 3 H), and −14.16 (dd, J_{PH} = 8.1 and 2 Hz, 1 H) ppm. $^{31}P\{^1H\}$ NMR ($CDCl_3$, 25 °C): 41.3 (d, 1 P) and 33.0 (d, 1 P) ppm, J_{PP} = 16 Hz.

Synthesis of $HFe_3(\mu\text{-}CNMe_2)(CO)_9(PPh_3)$. A solution of $HFe_3(\mu\text{-}CNMe_2)(CO)_{10}$ (12.4 mg, 0.0246 mmol) and PPh_3 (12.0 mg, 0.046 mmol) in cyclohexane (10 mL) in a 50-mL Schlenk flask was heated at 90 °C for 0.5 h under a nitrogen atmosphere. After evaporation of solvent by using a rotary evaporator the dark green residue was purified by thin-layer chromatography on silica gel with a cyclohexane/dichloromethane solution as the eluting agent (5:1 v/v). The bands in order of elution were purple $HFe_3(\mu\text{-}CNMe_2)(CO)_{10}$ (3.0 mg, 24%), dark green $HFe_3(\mu\text{-}CNMe_2)(CO)_9(PPh_3)$ (10.9 mg, 60%), and dark green $HFe_3(\mu\text{-}CNMe_2)(CO)_8(PPh_3)_2$ (3.5 mg, 15%).

$HFe_3(\mu\text{-}CNMe_2)(CO)_9(PPh_3)$. IR ($C_6H_{12}$): 2066 (m), 2018 (vs), 1995 (s), 1986 (s), 1980 (s), 1960 (w), 1949 (w), and 1921 (w) cm^{-1}. ^1H NMR (25 °C, $CDCl_3$): 7.3 (m, 15 H); b-e isomer (82%), 3.71 (s, 3 H), 2.89 (br s, 3 H), and −17.28 (d, J_{PH} = 16.1 Hz, 1 H) ppm; n-e isomer (18%), 3.78 (s, 6 H) and −16.90 (d, J_{PH} = 3.1 Hz, 1 H) ppm. $^{31}P\{^1H\}$ NMR (25 °C, $CDCl_3$): b-e isomer, 66.1 (s) ppm;

(6) Keister, J. B.; Payne, M. W.; Muscatella, M. J. *Organometallics* **1983**, *2*, 219.

(7) (a) Dalton, D. M.; Barnett, D. J.; Duggan, T. P.; Keister, J. B.; Malik, P. T.; Modi, S. P.; Shaffer, M. R.; Smesko, S. A. *Organometallics* **1985**, *4*, 1854. (b) Churchill, M. R.; Fettinger, J. C.; Keister, J. B. *Organometallics* **1985**, *4*, 1867.

(8) Howell, J. A. S.; Mathur, P. *J. Chem. Soc., Dalton Trans.* **1982**, 43.

(9) Churchill, M. R.; Lake, C. H.; Safarowic, F. J.; Parfitt, D. S.; Nevinger, L. R.; Keister, J. B. *Organometallics*, in press.

(10) Adams, R. D.; Babin, J. E.; Tanner, J. *Organometallics* **1988**, *7*, 765.

n-e isomer, 61.0 (s) ppm. $^{13}C\{^1H\}$ NMR (25 °C, $CDCl_3$): 327.9 (s, 1 C, CNR_2), 222.0 (s, 1 C), 218.1 (s, 1 C), 217.2 (s, 1 C), 214.3 (s, 1 C), 208.7 (s, 1 C), 53.3 (s, 1 C), and 50.9 (s, 1 C) ppm. Anal. Calcd for $H_{22}C_{30}O_9NPFe_3$: C, 48.76; H, 3.00. Found: C, 48.43; H, 3.05.

$HFe_3(\mu\text{-}CNMe_2)(CO)_8(PPh_3)_2$. IR ($C_6H_{12}$): 2065 (m), 2016 (s), 1990 (vs), 1980 (s sh), 1960 (m), and 1922 (w) cm^{-1}. ^1H NMR (25 °C, $CDCl_3$): 7.5 (br, 30 H), 3.58 (s, 3 H), 2.75 (s, 3 H), and −16.17 (dd, J_{PH} = 16 and 1 Hz, 1 H) ppm.

Kinetics of PPh_3 Substitution on $HFe_{3-n}Ru_n(\mu\text{-}CNMe_2)(CO)_{10}$. The substitution reactions were monitored by IR spectroscopy using a Beckman 4250 instrument. The samples were taken in 0.5-mm KBr solution cells. The reaction was monitored via the absorption at 2087 cm^{-1} for $HFe_3(\mu\text{-}CNMe_2)(CO)_{10}$ and at 2075 cm^{-1} for $HFeRu_2(\mu\text{-}CNMe_2)(CO)_{10}$. A 5.0-mL solution of the cluster (2–6 mM) and PPh_3 (lowest concentration, 2.8×10^{-2} M) in decane was placed in a jacketed reaction flask under nitrogen. The temperature was maintained with a Neslab constant-temperature circulating bath (±0.2 °C). Rate constants were determined by computer-calculated (program KINPLOT, written by Dr. R. Rusczcyk, formerly of the University at Buffalo) least-squares determination of the slope of the plot of ln (absorbance) vs time, over 3 half-lives. Three or four determinations were made for each set of conditions. The rate constants are reported as the mean for each set with error limits as the larger of the standard deviation ($n - 1$) or the 95% confidence limit for the least precise measurement of the set.

Results and Discussion

Metal fragment exchange is a proven, if usually inefficient, method of synthesis of mixed-metal clusters.[1] Syntheses of $HM_3(\mu\text{-}COMe)(CO)_{10}$ (M_3 = Ru_3, Os_3, Ru_2Os, $RuOs_2$) have been accomplished previously from the corresponding $M_3(CO)_{12}$,[2,6] but this method is rather inefficient for the mixed-metal clusters because of the difficulty of separation of the various components. The mixed-metal species $HFe_nRu_{3-n}(\mu\text{-}CX)(CO)_{10}$ (X = OMe, NMe_2) were synthesized by metal fragment exchange with homometallic $HM_3(\mu\text{-}CX)(CO)_{10}$.

$HFeRu_2(\mu\text{-}COMe)(CO)_{10}$. Pyrolysis of an equimolar mixture of $HFe_3(\mu\text{-}COMe)(CO)_{10}$ and $Ru_3(CO)_{12}$ yielded $HRu_3(\mu\text{-}COMe)(CO)_{10}$ as the only methylidyne-containing product.

On the other hand, pyrolysis of $HRu_3(\mu\text{-}COMe)(CO)_{10}$ and $Fe(CO)_5$ yielded one of the desired products, $HFeRu_2(\mu\text{-}COMe)(CO)_{10}$ (6% isolated yield, 14% based upon consumed starting material), which can be separated from unreacted $HRu_3(\mu\text{-}COMe)(CO)_{10}$ by careful thin-layer chromatography. The new cluster was characterized by IR, ^1H NMR, and mass spectrometry. The characterization is most readily made by comparison of the data to those of the homometallic analogs.[6,11] The composition is clearly indicated by the mass envelope of the molecular ion and subsequent fragmentation by loss of CO ligands. The IR spectrum in the 2150–1900-cm^{-1} region is considerably more complex than those of the more symmetrical homometallic clusters. The ^1H NMR spectrum indicates the presence of two isomers in solution, one of which (45%) displays a hydride resonance at −14.32 ppm, assigned to a hydride bridging the Ru–Ru edge because the chemical shift is similar to the value found for $HRu_3(\mu\text{-}COMe)(CO)_{10}$ (−14.89 ppm), and the other (55%) is at −16.85 ppm, assigned to a hydride bridging a Fe–Ru edge by comparison with the chemical shift of −18.20 ppm for the Fe analog. This is taken to indicate a mixture of the two isomers shown in Figure 1. A similar equilibrium between C_s and C_1 isomers was found for $HRu_{3-n}Os_n(\mu\text{-}COMe)(CO)_{10}$ (n =1, 2).[2]

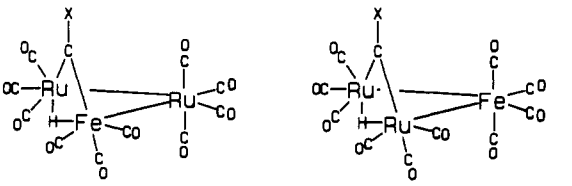

Figure 1. C_1 and C_s isomers for $HFeRu_2(\mu\text{-}CX)(CO)_{10}$ (X = OMe, NMe_2).

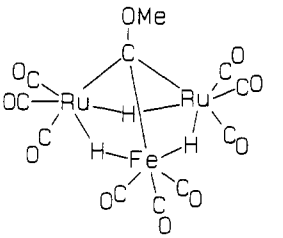

Figure 2. Proposed structure of $H_3FeRu_2(\mu_3\text{-}COMe)(CO)_9$.

$H_3FeRu_2(\mu\text{-}COMe)(CO)_9$. Analogs $HM_3(\mu\text{-}COMe)(CO)_{10}$, M_3 = Fe_3, $Ru_{3-n}Os_n$ (n = 0–3), react with hydrogen to form $H_3M_3(\mu_3\text{-}COMe)(CO)_9$; only the Fe_3 product is unstable with respect to elimination of hydrogen.[2,6]

Hydrogenation of $HFeRu_2(\mu\text{-}COMe)(CO)_{10}$ at 60 °C forms $H_3FeRu_2(\mu_3\text{-}COMe)(CO)_9$ (Figure 2) in very high yield. The product shows no tendency to lose hydrogen at room temperature. Characterization was achieved by IR, ^1H and ^{13}C NMR, and mass spectrometry. The EI mass spectrum displays the molecular ion and stepwise loss of CO ligands. The IR spectrum in the carbonyl region displays only terminal carbonyl absorptions and is more complex that the spectra of $H_3M_3(\mu_3\text{-}COMe)(CO)_9$, M = $Ru_{3-n}Os_n$ (n = 0–3), an indication of the much greater difference in electronic properties between Fe and Ru, compared with Ru and Os. The ^1H NMR spectrum displays the expected doublet at −20.05 and triplet at −18.08 ppm (J_{HH} = 3.0 Hz), compared with −17.53 for the Ru analog,[6] −23.57 ppm for $H_3Fe_3(\mu_3\text{-}CMe)(CO)_9$,[13] and −22.02 (d) and −21.15 (t, J = 5.3 Hz) ppm for $H_3Fe_3(\mu_3\text{-}COMe)(CO)_7(AsPh_3)_2$.[6] The $^{13}C\{^1H\}$ NMR spectrum for $H_3FeRu_2(\mu_3\text{-}COMe)(CO)_9$ shows resonances for all 11 carbons at room temperature. The resonances at 190.2 (2 C) and 190.0 (2 C) ppm are assigned to the two pairs of equatorial carbonyls on the Ru atoms, and the resonance at 191.2 (2 C) ppm is assigned to the axial carbonyl ligands on Ru (cf. equatorial (190.4 ppm) and axial (191.6 ppm) carbonyls of $H_3Ru_3(\mu_3\text{-}COMe)(CO)_9$). The resonances due to carbonyls bound to the iron are to lower field, as is expected.[13] The resonances at 207.0 (2 C) and 206.41 (1 C) ppm are assigned respectively to the equatorial and axial carbonyls on Fe. The methyl carbon resonance appears at 68.4 ppm, while the bridging methylidyne carbon resonance occurs at 266.5 ppm, compared with 252.0 ppm for the triruthenium analog.

It is of interest that $H_3FeRu_2(\mu_3\text{-}COMe)(CO)_9$ is stable with respect to loss of hydrogen under ambient conditions. $H_3Fe_3(\mu_3\text{-}COMe)(CO)_9$ reverts to $HFe_3(\mu\text{-}COMe)(CO)_{10}$ in the absence of hydrogen, although $H_3Fe_3(\mu_3\text{-}COMe)(CO)_7(AsPh_3)_2$ and $H_3Fe_3(\mu_3\text{-}CMe)(CO)_9$ are stable species. $H_3Ru_3(\mu_3\text{-}COMe)(CO)_9$ is an important starting point for the synthesis of other alkylidyne clusters $H_3Ru_3(\mu_3\text{-}CX)(CO)_9$ (X = H, Cl, Br, Ph, CO_2Me, SEt).[12] Therefore, $H_3FeRu_2(\mu_3\text{-}COMe)(CO)_9$, although available in low yield,

(11) Hodali, H. A.; Shriver, D. F. *Inorg. Chem.* **1979**, *18*, 1236.
(12) Keister, J. B. *Polyhedron* **1988**, *7*, 847.
(13) Dutta, T. K.; Meng, X.; Vites, J. C.; Fehlner, T. P. *Organometallics* **1987**, *6*, 2191.

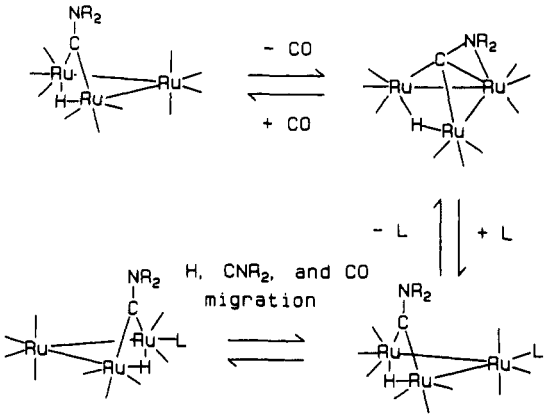

Figure 3. Proposed mechanism for substitution by PR_3 on $HRu_3(\mu\text{-}CNMe_2)(CO)_{10}$.

will allow for the synthesis of other iron diruthenium alkylidyne clusters.

$H_3FeRu_2(\mu_3\text{-}COMe)(CO)_9$ may be converted to $HFeRu_2(\mu\text{-}COMe)(CO)_{10}$ by reaction with CO at 55 °C for 2.5 h. These conditions are much milder than those required for the carbonylation of $H_3Ru_3(\mu_3\text{-}COMe)(CO)_9$. The rate of reaction, established by competitive carbonylation, is on the order of 20 times faster than that for the triruthenium analog, the order of relative rates for hydrogen elimination from $H_3M_3(\mu_3\text{-}COMe)(CO)_9$ being $M_3 = Fe_3 > FeRu_2 > Ru_3$.

$HFeRu_2(\mu\text{-}CNMe_2)(CO)_{10}$. Metal fragment exchange by pyrolysis of $Fe(CO)_5$ and $HRu_3(\mu\text{-}CNMe_2)(CO)_{10}$ was used to prepare $HFeRu_2(\mu\text{-}CNMe_2)(CO)_{10}$ in 18% yield, 51% based upon consumed starting material. The characterization is similar to that for the OMe analog. The mass spectrum displays the molecular ion and stepwise carbonyl and alkylidyne group loss, down to the bare trimetallic core. The ^1H NMR spectrum indicates predominately the isomer having local C_s symmetry. The hydride resonance at −14.29 ppm (s, 93%) is assigned to the hydride bridging the Ru–Ru bond of the C_s isomer, and the resonance at −16.47 ppm (s, 7%) is assigned to the Fe–H–Ru unit of the C_1 isomer. The resonances for the methyl groups appear at 3.84 ppm for the major isomer and at 3.98 ppm for the minor isomer.

The $^{13}C\{^1H\}$ NMR spectrum of $HFeRu_2(\mu\text{-}CNMe_2)(CO)_{10}$ displays fluxional behavior. The static spectrum at −60 °C contains resonances at 210.5 (2 C) ppm, assigned to the equatorial CO ligands on Fe, and 220.9 (1 C) and 220.0 (1 C) ppm, assigned to the axial CO ligands on Fe, and RuCO resonances at 199.9 (2 C), 197.0 (2 C), and 191.0 (2 C) ppm. The bridging carbon resonance appears at 306.4 ppm. The methyl resonance is at 54.7 ppm. The ^{13}C NMR spectrum at 25 °C shows carbonyl resonances due to three pairs of CO ligands on the Ru atoms, while the resonances due to the CO ligands on Fe are exchange broadened. Similar fluxionality for the $M(CO)_4$ fragment is found for $HRu_3(\mu\text{-}COMe)(CO)_{10}$ and for $HRu_2Os(\mu\text{-}COMe)(CO)_{10}$.[2]

Ligand Substitution on $HM_3(\mu\text{-}CNMe_2)(CO)_{10}$ (M_3 = Fe_3, $FeRu_2$). In earlier work it was shown that substitution by PPh_3 on $HRu_3(\mu\text{-}CNMe_2)(CO)_{10}$ occurred by a dissociative mechanism, with the initial site of substitution an equatorial coordination site on the nonbridged metal atom (n-e site); however, an intramolecular rearrangement produced an equilibrium mixture also containing the more stable isomer which is substituted in an equatorial site on a bridged metal atom (b-e site).[7,14] The proposed mechanism is shown in Figure 3.

(14) Shaffer, M. R.; Keister, J. B. *Organometallics* **1986**, *5*, 561.

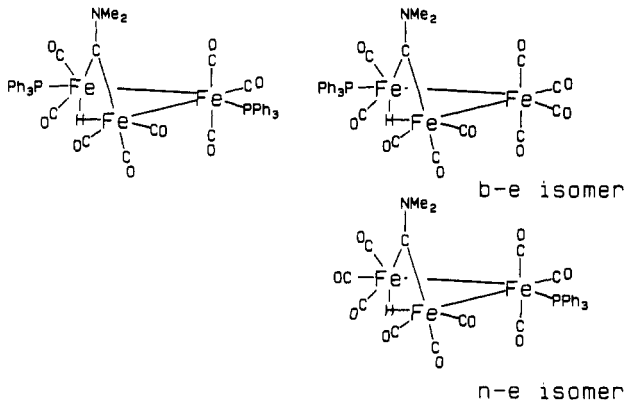

Figure 4. Proposed structures of $HFe_3(\mu\text{-}CNMe_2)(CO)_{10-n}(PPh_3)_n$ (n = 1, 2).

Hydrogenation of $HM_3(\mu\text{-}COMe)(CO)_{10}$ also occurs via a dissociative mechanism, with the relative rates for CO dissociation being Ru_3 (4500) > Ru_2Os (1100) > $RuOs_2$ (220) ≫ Os_3 (1).[2,15,16] In this series the reactivities of the mixed-metal clusters were intermediate between the reactivities of the two homometallic clusters.

Thus, the behavior of the $HM_3(\mu\text{-}CNMe_2)(CO)_{10}$ (M_3 = Fe_3, $FeRu_2$, Ru_3) series provided an excellent opportunity to investigate the unusual reactivity of mixed Fe/Ru clusters since the mechanism of substitution appeared to be well understood for the Ru_3 cluster and since all these species are isostructural.

In order to compare the mixed-metal cluster with both Fe_3 and Ru_3 analogs, we first investigated the ligand substitution on $HFe_3(\mu\text{-}CNMe_2)(CO)_{10}$. Reaction with 1 equiv of PPh_3 gave predominantly $HFe_3(\mu\text{-}CNMe_2)(CO)_9(PPh_3)$ and also $HFe_3(CNMe_2)(CO)_8(PPh_3)_2$. Characterizations of the products are straightforward by comparison of the IR and ^1H and ^{31}P NMR data with those of the Ru analogs.[7]

The monosubstituted product exists in solution as a mixture of n-e and b-e isomers (Figure 4). The ^1H–^{31}P coupling constants are characteristic. For $HRu_3(\mu\text{-}CNR_2)(CO)_9(PR'_3)$ n-e-substituted isomers display hydride–^{31}P coupling constants of ca. 2–3 Hz, while b-e isomers exhibit coupling constants of 7–10 Hz.[5] Coupling constants for Fe clusters are somewhat larger than those for the Ru clusters. The major isomer of $HFe_3(\mu\text{-}CNMe_2)(CO)_9(PPh_3)$ (82%) displays a hydride resonance at −17.26 (d) ppm with J_{HP} = 15.1 Hz, characteristic for b-e substitution by PPh_3. The minor isomer (18%) displays a hydride resonance characteristic for n-e coordination (−16.87 (d) ppm, J_{HP} = 3.1 Hz). The ^{31}P NMR resonances for the b-e and n-e isomers are 66.14 and 60.97 ppm, respectively. For comparison, b-e and n-e isomers of $HRu_3(\mu\text{-}CNMe_2)(CO)_9(PPh_3)$ display resonances at 39.10 and 36.98 ppm, respectively.

The disubstituted cluster is the ultimate product in the presence of a large excess of PPh_3, as it precipitates from hydrocarbon solution. The structure is shown in Figure 4. The doublet of doublets hydride resonance indicates that one PPh_3 ligand is coordinated in a b-e site (J_{PH} = 16 Hz) and the second in a n-e site (J_{PH} = 1 Hz), as is the case for the Ru_3 analog.[7] In the absence of excess PPh_3, $HFe_3(\mu\text{-}CNMe_2)(CO)_8(PPh_3)_2$ decomposes to $HFe_3(\mu\text{-}CNMe_2)(CO)_9(PPh_3)$.

(15) Shojaie, R.; Atwood, J. D. *Inorg. Chem.* **1988**, *27*, 2558.
(16) (a) Bavaro, L. M.; Montangero, P.; Keister, J. B. *J. Am. Chem. Soc.* **1983**, *105*, 4977. (b) Bavaro, L. M.; Keister, J. B. *J. Organomet. Chem.* **1985**, *287*, 357. (c) Anhaus, J.; Bajaj, H. C.; van Eldik, R.; Nevinger, L. R.; Keister, J. B. *Organometallics* **1989**, *8*, 2903.

Table I. Pseudo-First-Order Rate Constants for the Substitution on $HFe_3(\mu\text{-}CNMe_2)(CO)_{10}$ by PPh_3

T (°C)	$[PPh_3]$ (mM)	10^4k_{obs} (s^{-1})	T (°C)	$[PPh_3]$ (mM)	10^4k_{obs} (s^{-1})
30.0	28	0.130 (0.016)	40.0	56	0.50 (0.10)
40.0	28	0.46 (0.08)	50.0	28	1.81 (0.14)
40.0	28	0.25 (0.04)[a]	60.0	28	8.7 (1.6)

[a] Under 1 atm of CO.

The kinetics of the first ligand substitution under pseudo-first-order conditions were also investigated. During the course of reaction the color of the solution changes from purple, the color of $HFe_3(\mu\text{-}CNMe_2)(CO)_{10}$, to an olive green. The only substituted product was the olive green disubstituted cluster $HFe_3(\mu\text{-}CNMe_2)(CO)_8(PPh_3)_2$, which precipitates from solution. The rate law for disappearance of $HFe_3(\mu\text{-}CNMe_2)(CO)_{10}$ was found to be first order in $[HFe_3(CNMe_2)(CO)_{10}]$ and zero order in $[PPh_3]$ over a small concentration range, consistent with a CO dissociative mechanism. The initial rate was inhibited by the presence of a CO atmosphere, but since the reaction is reversible, this does not provide conclusive evidence for a CO dissociative mechanism. Decomposition of the cluster during extended treatment with CO prevented us from obtaining equilibrium constants. Rate constants are given in Table I. The activation enthalpy was determined to be $\Delta H^\ddagger$ = 114 (±10) kJ/mol (27.4 (±2.3) kcal/mol), and the activation entropy was $\Delta S^\ddagger$ = +40 (±30) J/K·mol (+9 (±7) cal/K·mol). These data are quite similar to data for analogous substitutions on $HRu_3(\mu\text{-}CX)(CO)_{10}$ (X = NMe_2, $\Delta H^\ddagger$ = 26.9 kcal/mol, $\Delta S^\ddagger$ = +3 cal/K·mol; X = OMe, $\Delta H^\ddagger$ = 26.6 kcal/mol, $\Delta S^\ddagger$ = +8 cal/K·mol), which appear to occur via CO dissociative mechanisms.[7a,c] Although other intramolecular activated complexes may be postulated, the data are consistent with CO dissociation as the rate-determining step.

Substitution by PPh_3 on $HFeRu_2(\mu\text{-}CNMe_2)(CO)_{10}$. The reaction of 1 equiv of PPh_3 with $HFeRu_2(\mu\text{-}CNMe_2)(CO)_{10}$ in hydrocarbon solution at room temperature overnight or at 40–60 °C for several hours gave as the major product $HFeRu_2(\mu\text{-}CNMe_2)(CO)_9(PPh_3)$ in greater than 65% yield. There were small amounts of $HRu_3(\mu\text{-}CNMe_2)(CO)_{10}$ and $HRu_3(\mu\text{-}CNMe_2)(CO)_9(PPh_3)$ produced as well. Fragmentation is more important for first-row transition-metal clusters than for second- and third-row metals; we have shown previously that the cluster core is retained during interconversion of $HRu_{3-n}Os_n(\mu\text{-}COMe)(CO)_{10}$ and $H_3Ru_{3-n}Os_n(\mu_3\text{-}COMe)(CO)_9$. Still, only 26% of the products are due to fragmentation, and thus fragmentation does not in itself account for the higher rate of disappearance for $HFeRu_2(\mu\text{-}CNMe_2)(CO)_{10}$, compared with $HM_3(\mu\text{-}CNMe_2)(CO)_{10}$ (M = Fe, Ru) in their substitution reactions.

The monosubstituted product $HFeRu_2(\mu\text{-}CNMe_2)(CO)_9(PPh_3)$ exists as only one isomer in solution. On the basis of the ^1H and ^{31}P NMR data, this compound appears to be substituted in a b-e position on Ru, with Fe in the nonbridged site; this assignment is based upon the hydride–^{31}P coupling constant (8.1 Hz), which indicates b-e substitution, the hydride chemical shift of −13.76 ppm, indicating that both Ru atoms are bridged, and also the ^{31}P chemical shift of 41.5 ppm, indicating substitution on Ru. Thus, the geometry of the metal core of the major isomer of $HFeRu_2(\mu\text{-}CNMe_2)(CO)_{10}$ is maintained upon substitution. The $^{13}C\{^1H\}$ NMR spectrum of $HFeRu_2(\mu\text{-}CNMe_2)(CO)_9(PPh_3)$ at room temperature contains peaks at 200.8 (s, 1 C), 198.4 (s, 1 C), and 190.2 (s, 1 C) ppm that correspond to the three carbonyls of the $Ru(CO)_3$ unit (cf. 201.7, 197.9, and 189.9 ppm for the analogous carbonyls of $HRu_3(\mu\text{-}CNMe_2)(CO)_9(PPh_3)$). Two doublets at 206.6 (d, 1 C, J_{CP} = 10 Hz) and 202.0 (d, 1 C, J_{CP} = 7 Hz) ppm are assigned to the carbonyls on the substituted Ru center (cf. 207.5 ppm (d, J_{CP} = 9 Hz) and 201.6 ppm (d, J_{CP} = 4 Hz), for the $Ru(CO)_2(PPh_3)$ ligands of $HRu_3(\mu\text{-}CNMe_2)(CO)_9(PPh_3)$ trans to $CNMe_2$ and H, respectively). The resonances for the *N*-methyl groups are at 54.1 and 52.1 ppm. The methylidyne carbon was observed as a singlet at 317.2 ppm (cf. 318.6 ppm for $HRu_3(\mu\text{-}CNMe_2)(CO)_9(PPh_3)$) and the chemical shift is slightly downfield from that of the methylidyne carbon in the unsubstituted cluster. The four carbonyls bound to Fe are not observed at room temperature due to fluxional broadening, but at −60 °C resonances due to these ligands appear at 210.0 (equatorial CO), 220.2 (equatorial CO), 222.4 (axial CO), and 228.7 (axial CO) ppm.

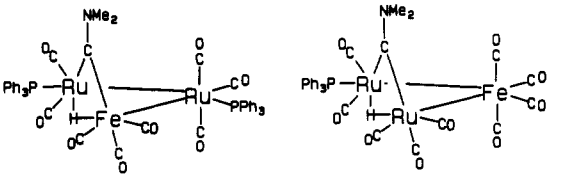

Figure 5. Proposed structures of $HFeRu_2(\mu\text{-}CNMe_2)(CO)_9(PPh_3)$ and $HFeRu_2(\mu\text{-}CNMe_2)(CO)_8(PPh_3)_2$.

Table II. Rate Constants for Substitution by PPh_3 on $HFeRu_2(\mu\text{-}CNMe_2)(CO)_{10}$

T (°C)	$[PPh_3]$ (mM)	10^4k_{obs} (s^{-1})	T (°C)	$[PPh_3]$ (mM)	10^4k_{obs} (s^{-1})
40.0	44	3.1 (0.3)	40.0	44	1.3 (0.2)[a]
40.0	80	3.2 (0.3)			

[a] Under 1 atm of CO.

Table III. Rate Constants at 40 °C for Substitution by PPh_3 on $HFe_{3-n}Ru_n(\mu\text{-}CNMe_2)(CO)_{10}$

cluster	10^5k (s^{-1})	cluster	10^5k (s^{-1})
Ru_2Fe	31	Ru_3	0.57
Fe_3	4.8		

Another product formed in this substitution reaction was $HFeRu_2(\mu\text{-}CNMe_2)(CO)_8(PPh_3)_2$. The ^1H NMR spectrum displays a doublet of doublets at −14.17 ppm with phosphorus–hydride coupling constants of 8 and 1–2 Hz. The larger coupling constant is due to a PPh_3 ligand in a b-e site, while the smaller coupling constant is consistent with a second phosphine coordinated in a n-e site, as was fouind for $HRu_3(\mu\text{-}CNRR')(CO)_8(PPh_3)_2$.[7] The ^{31}P NMR spectrum for the disubstituted product shows two doublets at 41.3 and 33.0 ppm (J_{PP} = 16 Hz). ^{31}P NMR spectra of the homometallic clusters show that phosphines bound to ruthenium have chemical shifts in the 30–45 ppm range and phosphines bound to iron have chemical shifts in the 60–70 ppm range. Some examples are $HRu_3(\mu\text{-}CNMe_2)(CO)_9(PPh_3)$ (39.10 ppm, major isomer, phosphine in bridged-equatorial position, and 36.98 ppm, minor isomer, phosphine in nonbridged-equatorial position) and $HRu_3(\mu\text{-}CNBz_2)(CO)_9(PPh_3)$ (37.11 ppm, phosphine in the nonbridged-equatorial position); for $HFe_3(\mu\text{-}CNMe_2)(CO)_9(PPh_3)$ the ^{31}P NMR resonances for the b-e and n-e isomers are 66.14 and 60.97 ppm, respectively. These NMR data prove that the disubstituted product has one phosphine bound to a ruthenium in a n-e site and a second phosphine bound to a ruthenium in a b-e site (Figure 5).

The kinetics of the substitution reaction were determined. Because of the small quantities of mixed-metal cluster available, the studies were more limited than those on the homometallic analogs. Pseudo-first-order rate

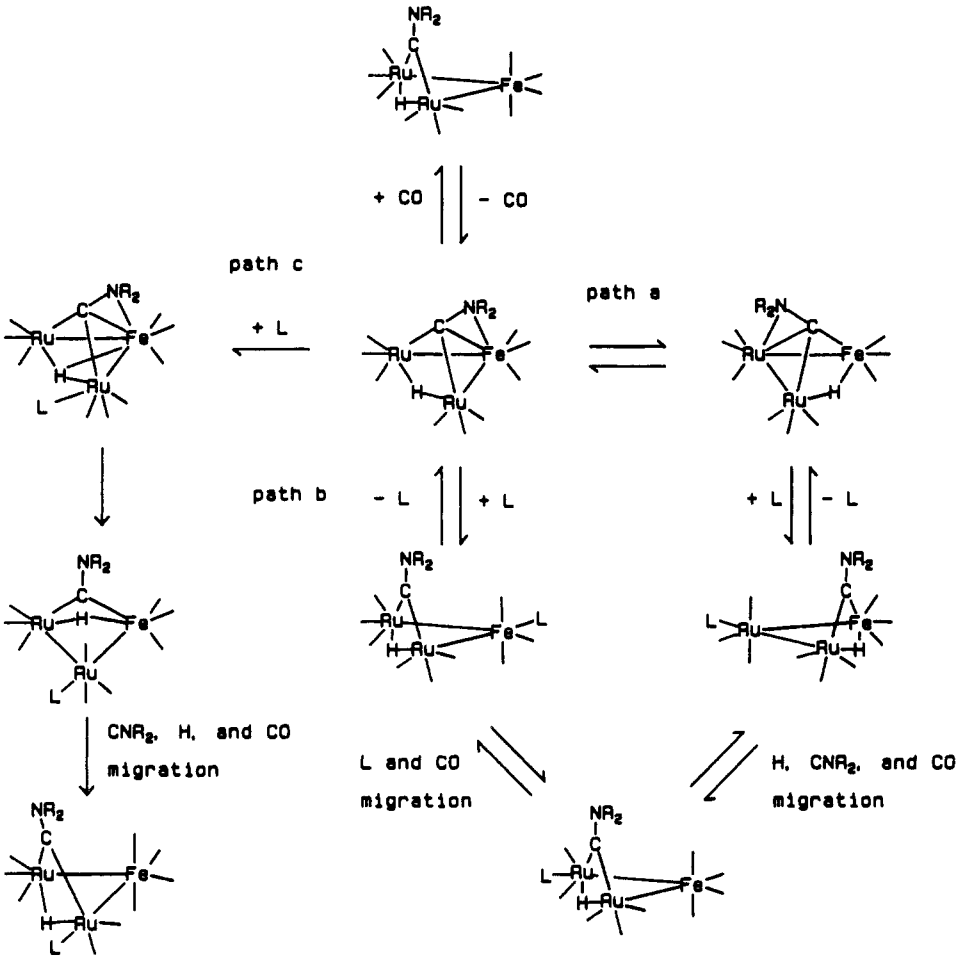

Figure 6. Possible mechanism for substitution by PPh_3 on $HFeRu_2(\mu\text{-}CNMe_2)(CO)_{10}$.

constants are provided in Table II. The rate of reaction was found to be first order with respect to $[HFeRu_2(CNMe_2)(CO)_{10}]$ and independent of $[PPh_3]$ over the small concentration range investigated. The reaction was inhibited under a CO atmosphere. Heating $HFeRu_2(CNMe_2)(CO)_9(PPh_3)$ under CO led to cluster fragmentation; thus, the CO inhibition suggests a CO dissociative rate-determining step.

The structures of the substitution products $HFeRu_2(\mu\text{-}CNMe_2)(CO)_{10-n}(PPh_3)_n$ suggest that CO dissociation could occur from Ru. However, the rate constant for substitution, 3.1×10^{-4} s^{-1} at 40 °C, is only 7 times greater than the rate constant for the Fe_3 analog and 54 times greater than that for the Ru_3 analog, even though the observed product is substituted on a Ru atom. This is more consistent with a mechanism in which CO dissociation occurs from Fe.

Possible Mechanisms. The mechanisms for substitution for CO by PPh_3 on $HFe_{3-n}Ru_n(\mu\text{-}CNMe_2)(CO)_{10}$ and on $Fe_{3-n}Ru_n(CO)_{12}$ are dissociative, as shown by the first-order rate laws, positive entropies of activation, and inhibition by CO (although not conclusively for $HFe_3(\mu\text{-}CNMe_2)(CO)_{10}$). For both series, the order of relative rates, $FeRu_2 > Fe_3 > Ru_3$, suggests that CO dissociation occurs from Fe in the mixed-metal clusters, but in all cases the site of PPh_3 substitution is on a Ru atom. There is no requirement that the site of addition of PPh_3 be the same as the site for CO dissociation.

On the basis of previous studies involving $HRu_3(\mu\text{-}CNMe_2)(CO)_{10}$, we assume that CO dissociation is most rapid from the Fe atom in the nonbridged site, the predominant isomer for $HFeRu_2(\mu\text{-}CNMe_2)(CO)_{10}$. For the Ru_3 cluster, PPh_3 adds to the same metal center in the nonbridged site, and intramolecular rearrangement forms an equilibrium mixture of b-e and n-e isomers. For $HRu_3(\mu\text{-}CNMe_2)(CO)_{10}$ the rearrangement was proposed to involve migration of hydride, methylidyne, and carbonyl ligands, but the PPh_3 ligand was proposed to remain attached to the same metal atom throughout the isomerization.[14]

For the $FeRu_2$ cluster, PPh_3 addition cannot occur in this way. Assuming that the first intermediate formed by CO dissociation contains Fe in the nonbridged site, then there are a number of possible mechanisms which must be considered for the subsequent steps: (1) the initial product may be substituted on Fe but PPh_3 dissociation may be more rapid than CO dissociation, allowing a dissociative pathway for n-e → b-e Ru isomerization which is not found for the Ru_3 analog; (2) the intermediate may isomerize to place Ru in the unique site, which is then attacked by PPh_3; (3) PPh_3 attack may occur at Fe, but intramolecular migration of CO and PPh_3 may generate the observed product; (4) attack by PPh_3 may occur directly at an Ru atom bridged by the hydride.

Mechanism 1. Dissociative Isomerization. Unlike the Ru_3 analog, PPh_3 dissociation from $HFe_3(\mu\text{-}CNMe_2)(CO)_9(PPh_3)$ occurs under the reaction conditions at 40 °C. Therefore, it is possible that, for the mixed-metal cluster, the initial site for CO dissociation and PPh_3 addition is the Fe center but that the rate of PPh_3 dissociation from the Fe center is much faster than from the more stable product finally isolated. Since we have been unable to isolate the isomer in which PPh_3 substitution has occurred on Fe, this hypothesis remains to be proven.

However, the rate constant for replacement of PPh_3 on $HFe_3(\mu\text{-}CNMe_2)(CO)_9(PPh_3)$ by CO (1 atm, k_{obs} ca. 1×10^{-4} s^{-1} at 40 °C) is on the same order as that for CO dissociation from $HFe_3(\mu\text{-}CNMe_2)(CO)_{10}$. If the relative rates of ligand dissociation from the Fe center of $HFeRu_2(\mu\text{-}CNMe_2)(CO)_9L$ (L = CO, PPh_3) are similar to those from the Fe_3 analog, then this mechanism is ruled out because a significant quantity of the Fe-substituted isomer should be observed during the reaction if the rate constants for PPh_3 substitution on Fe and PPh_3 dissociation from Fe are comparable.

Mechanism 2 (Figure 6, Path a). Isomerization of the intermediate $HFeRu_2(\mu\text{-}CNMe_2)(CO)_9$ occurs to place Ru in the unique position. The C_1 and Cs isomers of $HFeRu_2(\mu\text{-}CX)(CO)_{10}$ are in equilibrium, and it would not be surprising if isomerization of the intermediate is also rapid. Attack by PPh_3 on the Ru atom of the less stable C_1 isomer may be preferred on steric grounds.

Mechanism 3 (Figure 6, Path b). Attack by PPh_3 at the Fe atom generates $HFeRu_2(\mu\text{-}CNMe_2)(CO)_9(PPh_3)$ with substitution on Fe in the n-e site. Migration by PPh_3 to Ru and by CO from Ru to Fe would then generate the observed b-e product substituted on Ru. Precedent for phosphine migration has been recently provided by Puddephatt;[17] PR_3 ligands have been found to undergo rapid intramolecular migrations between the three Pt atoms of $[Pt_3(\mu_3\text{-}CO)(\mu\text{-}PPh_2CH_2PPh_2)_3(PR_3)]^+$. However, PR_3 intrametallic migration has not been observed in saturated cluster systems. Furthermore, the close similarity between the rate constants for n-e → b-e isomerizations of $HRu_3(\mu\text{-}CNMe_2)(CO)_9(ER_3)$ (E = P, As, Sb) suggests that ER_3/CO intramolecular, intermetallic exchange is not involved in the mechanism.[14]

Mechanism 4 (Figure 6, Path c). If the structure of the intermediate retains the C_s symmetry of the $HM_3(\mu\text{-}CNMe_2)$ core, attack by PPh_3 might occur directly on one of the bridged Ru atoms, concomitant with hydride and methylidyne migration, to generate the n-e-substituted isomer, which could then rearrange to the preferred b-e isomer. Presumably, the same mechanism would then apply for substitution on $HRu_3(CNMe_2)(CO)_{10}$.

At this time we have no basis for distinction among mechanisms 2–4. All of these include intramolecular, intermetallic ligand migrations. Such migrations have also been proposed in a number of earlier studies of substitution on mixed-metal clusters. Atwood and Shojaie invoked CO migration to account for the ligand substitution behavior of $Ru_{3-n}Fe_n(CO)_{12}$.[3] Unsaturated intermediates containing bridging CO ligands, for example, $MnRe(CO)_9$,[18] $CpMoMn(CO)_7$,[19] and $Ru_3(CO)_{11}$,[20] have been identified by matrix isolation studies. It is becoming apparent that unsaturated metal cluster intermediates frequently contain bridging ligands or undergo facile rearrangements, making the reactive metal site difficult to identify. Studies of mixed-metal clusters are necessary to reveal these complicating mechanistic features.

Acknowledgment. This work was supported by Grant CHE8900921 from the National Science Foundation.

OM9202783

(17) Bradford, A. M.; Douglas, G.; Manojlovic-Muir, L.; Muir, K. W.; Puddephatt, R. J. *Organometallics* **1990**, *9*, 409.

(18) Firth, S.; Hodges, P. M.; Poliakoff, M.; Turner, J. J. *Inorg. Chem.* **1986**, *25*, 4608.

(19) Pope, K. R.; Wrighton, M. S. *Inorg. Chem.* **1987**, *26*, 2321.

(20) Bentsen, J. G.; Wrighton, M. S. *J. Am. Chem. Soc.* **1987**, *109*, 4530.

Structure and Bonding in Bis(stannylene) Adducts of Zirconocene and 1,1′-Dimethylzirconocene

Warren E. Piers,*[1] Randy M. Whittal,[1] George Ferguson,[1] John F. Gallagher,[1] Robert D. J. Froese,[1] Henry J. Stronks,[2] and Peter H. Krygsman[2]

Guelph-Waterloo Centre for Graduate Work in Chemistry, Guelph Campus, Department of Chemistry and Biochemistry, University of Guelph, Guelph, Ontario, Canada N1G 2W1, and Bruker Spectrospin (Canada) Ltd., 555 Steeles Avenue East, Milton, Ontario, Canada L9T 1Y6

Received July 28, 1992

Decomposition of in situ generated $Cp'_2Zr(n\text{-}Bu)_2$ in the presence of 2 equiv of Lappert's stannylene $Sn[CH(SiMe_3)_2]_2$ yields the products $Cp'_2Zr\{Sn[CH(SiMe_3)_2]_2\}_2$ (Cp′ = C_5H_5 (**1a**, 42%), $C_5H_4CH_3$ (**1b**, 52%)). The ^{119}Sn NMR resonance for **1a** appears at +1677.6 ppm relative to Me_4Sn, with satellites arising from coupling to an adjacent ^{117}Sn nucleus ($^2J_{^{117}Sn}$ = 630 Hz). The compound **1b** was the subject of a single-crystal X-ray structure determination. It crystallizes in the space group $C2/c$ (No. 15) with a = 25.455 (14) Å, b = 11.563 (3) Å, c = 19.471 (11) Å, β = 93.46 (5)°, V = 5721 (5) Å^3, and Z = 4. Refinement of 231 variables on 3529 reflections observed ($I > 3.0\sigma(I)$) converged to R = 0.048 and R_w = 0.072. The molecule has pseudotetrahedral geometry at the zirconium atom with a 2-fold axis bisecting the Cp–Zr–Cp and Sn–Zr–Sn angles, two equivalent Zr–Sn bonds of 2.8715 (11) Å, and an Sn–Sn separation of 4.236 Å. Extended Hückel molecular orbital calculations show that there is significant π bonding between zirconium and tin in these complexes.

Introduction

Unearthing new examples of the periodicity inherent in the chemistry of the elements of the periodic table is a never-ending source of delight for chemists of all subdisciplines. Particularly striking are the parallels between the organometallic chemistry of the early transition metals and their corresponding groups in the p block of the periodic table. For example, a strong connection exists between organoscandium and organoaluminum chemistry;[3]

(1) Guelph-Waterloo Centre for Graduate Work in Chemistry, Guelph Campus.

(2) Bruker Spectrospin (Canada) Ltd.

(3) Piers, W. E.; Shapiro, P. J.; Bunel, E. E.; Bercaw, J. E. *Synlett.* **1990**, *1*, 74.

0276-7333/92/2311-4015$03.00/0